JOURNAL OF AGRICULTURAL AND FOOD CHEMISTRY

Article

Cite This: J. Agric. Food Chem. 2019, 67, 6962−6969

pubs.acs.org/JAFC

Sulfone-Based Probes Unraveled Dihydrolipoamide *S*-Succinyltransferase as an Unprecedented Target in Phytopathogens

Biao Chen,[†] Qingsu Long,[†] Yongliang Zhao,[†] Yuanyuan Wu,[†] Shasha Ge,[†] Peiyi Wang,[†] Cai-Guang Yang,[‡] Yonggui Chi,[†] Baoan Song,*[,†] and Song Yang*[,†,§]

[†]Laboratory Breeding Base of Green Pesticide and Agricultural Bioengineering, Key Laboratory of Green Pesticide and Agricultural Bioengineering, Ministry of Education, Guizhou University, Huaxi District, Guiyang, Guizhou 550025, People's Republic of China

[‡]Laboratory of Chemical Biology, State Key Laboratory of Drug Research, Shanghai Institute of Materia Medica, Chinese Academy of Sciences, Shanghai 201203, People's Republic of China

[§]College of Pharmacy, East China University of Science & Technology, Shanghai 200237, People's Republic of China

Supporting Information

ABSTRACT: Target validation of current drugs remains the major challenge for target-based drug discovery, especially for agrochemical discovery. The bactericide **0** represents a novel lead structure and has shown potent efficacy against those diseases that are extremely difficult to control, such as rice bacterial leaf blight. However, no detailed target analysis of this bactericide has been reported. Here, we developed a panel of **0**-derived probes **1**−**6**, in which a conservative modification (alkyne tag) was introduced to keep the antibacterial activity of **0** and provide functionality for target identification via click chemistry. With these cell-permeable probes, we were able to discover dihydrolipoamide *S*-succinyltransferase (DLST) as an unprecedented target in living cells. The probes showed good preference for DLST, especially probe **1**, which demonstrated distinct selectivity and reactivity. Also, we reported **0** as the first covalent DLST inhibitor, which has been used to confirm the involvement of DLST in the regulation of energy production.

KEYWORDS: *bactericide **0**, target, DLST, covalent inhibitor, energy production*

1. INTRODUCTION

Since the late 19th century, crop protection chemistry has become a high-tech science in supporting the sustainable production of food from available farmland.[1] Advancements in the discovery of highly effective agrochemicals will be required to tackle the challenge of increasing food production. Generally, the discovery of a commercialized agrochemical will take about 10 years at a cost of approximately U.S. $286 million and a screening of above 150 000 compounds.[2] An important step that accelerates the agrochemical discovery process is to enlarge the number of druggable targets as well as to deeply understand the molecular and cellular mechanism of action of current agrochemicals. With a known target, multiple techniques, such as crystallography, computational modeling, biochemistry, and binding kinetics, can be used to analyze the target interaction with drugs, enabling efficient target-based drug design.[3] However, target validation of current drugs remains the major challenge for target-based drug discovery, especially for agrochemical discovery. The definite mechanism of most agrochemicals is unclear, which results in so few targets that can be used for target-based molecular design.

Bacterial plant pathogens, especially the top 10,[4] severely infect a number of economically important crops and seriously reduce the crop yield. The bacterial outbreaks are generally difficult to control as a result of the lack of effective bactericides and the increasing resistance problem, thereby emphasizing an urgent demand for the discovery of new antibacterial agents. The sulfone reagents represent promising biologically active privileged structures that can react covalently with the active sites of certain proteins.[5−7] Among them, the drug candidate **0** (jiahuangxianjunzuo, in registration stage) and its analogues have been reported to show potent efficacy against those diseases[8−12] that are extremely difficult to control, such as *Xanthomonas oryzae* pv. *oryzae* (*Xoo*) and *Xanthomonas axonopodis* pv. *citri* (*Xac*). However, no detailed target analysis of this bactericide has been conducted thus far in living systems.

Recently, an unbiased chemical proteomic strategy termed "activity-based protein profiling" (ABPP)[13−15] has been used as a powerful method for the target deconvolution of bioactive molecules. ABPP used activity-site-directed probes to profile the functional state of enzymes directly in native biological systems, which has been developed for multiple enzyme classes, such as cysteine proteases, serine hydrolases, phosphatases, and kinases.[16] To investigate the interactions between **0** and its protein targets in bacteria, we designed a series of alkyne-functionalized probes **1**−**6** (Figure 1A) and systematically evaluated their reactivity and selectivity directly in living bacterial cells. As expected, a minor change in a common structure resulted in a selective labeling event of a ∼45 kDa

Received: April 2, 2019
Revised: May 27, 2019
Accepted: May 31, 2019
Published: May 31, 2019

DOI: 10.1021/acs.jafc.9b02059
J. Agric. Food Chem. 2019, 67, 6962−6969

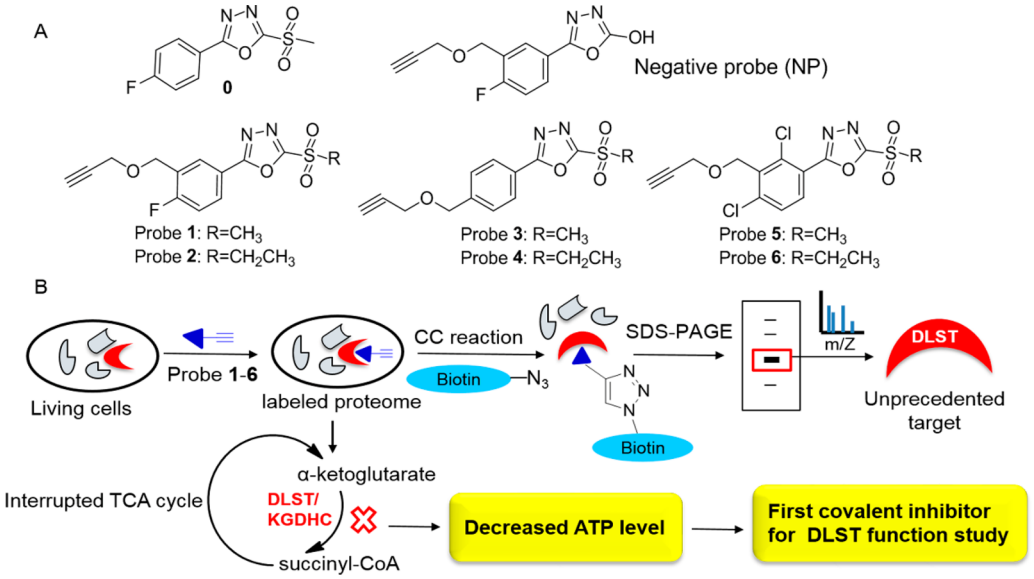

Figure 1. Design of **0**-derived probes. (A) Chemical structures of **0** and its clickable analogues. (B) Detection and identification of the probe-labeled proteome by the ABPP strategy.

protein. All probes containing an alkyne handle were used for the modification with a reporter group (e.g., biotin) via the 1,3-dipolar Huisgen cycloaddition [click chemistry (CC)] after cell penetration and lysis.[17,18] Labeled proteins are separated by sodium dodecyl sulfate (SDS) gels, visualized by streptavidin blot, and subsequently identified by mass spectrometry (Figure 1B).[19]

2. MATERIALS AND METHODS

2.1. Instruments and Chemicals. ^{1}H and ^{13}C nuclear magnetic resonance (NMR) spectral analyses were performed on a JEOL-ECX 500 NMR spectrometer using $CDCl_3$ or DMSO-d_6 as the solvent and tetramethylsilane (TMS) as an internal standard. High-resolution mass spectrometry (HRMS) was conducted on a LTQ Orbitrap (Thermo Scientific). Imaging analysis was conducted on the ChemiDoc XRS+ system (Bio-Rad). All reagents from the Chinese Chemical Reagent Company were reagent-grade and used without further purification.

2.2. General Synthetic Procedures for the Intermediates 1−6. The intermediates **1**−**4** were prepared according to previously reported methods.[8] Thioether derivative **4** was prepared by esterification, hydrazidation, cyclization, and thioetherification reactions. To a solution of intermediate **4** (0.03 mol) in 50 mL of CCl_4 was added *N*-bromosuccinimide (0.036 mol) and a catalytic amount of azobis(isobutyronitrile) (AIBN, 0.003 mol). The mixture was refluxed for 48 h, and then CCl_4 was evaporated to obtain the crude product, which was further washed with saturated aqueous $NaHCO_3$ and dried over Na_2SO_4. The organic layer was evaporated, and the residue was purified by silica gel column chromatography to obtain the intermediates **5a**−**5f** with yields of 43−77%. To a solution of intermediate **5** (5 mmol) and propargyl alcohol (5.1 mmol) in 20 mL of dried dimethylformamide (DMF), 60% sodium hydride (6 mmol) was added. The reaction was stirred for 2 h under an ice bath. The mixture was quenched by adding saturated NH_4Cl (aqueous) and extracted by ethyl acetate. The organic layer was washed with saturated NH_4Cl 2 times, dried over Na_2SO_4, and filtered, and the solvent was removed under reduced pressure. The crude product was purified by silica gel column chromatography to obtain the intermediates **6a**−**6f** with yields of 43−66%.

2.3. General Synthetic Procedures for the Probes 1−6. To a stirred solution of intermediate **6** (5 mmol) in 15 mL of CH_2Cl_2 was added 3-chloroperbenzoic acid (m-CPBA, 15 mmol). The reaction was stirred for 2 h, and the mixture was filtered. After evaporation, the obtained crude product was purified by silica gel column chromatography with ethyl acetate/petroleum ether (1:6, v/v) to give the pure probes **1**−**6** with yields of 40−70%. The representative data for probe **1** are presented below.

2-(Methylsulfonyl)-5-(4-fluoro-3-((prop-2-yn-1-yloxy)methyl)-phenyl)-1,3,4-oxadiazole (probe **1**): yield, 70%; white solid; ^{1}H NMR (500 MHz, $CDCl_3$), δ 8.26 (dd, J = 6.6 and 2.2 Hz, 1H, Ph−6H), 8.10 (m, 1H, Ph−2H), 7.25 (t, J = 8.9 Hz, 1H, Ph−5H), 4.74 (s, 2H, Ph−CH_2O−), 4.30 (d, J = 2.4 Hz, 2H, −OCH_2−C≡CH), 3.53 (s, 3H, −SO_2CH_3), 2.52 (t, J = 2.4 Hz, 1H, −C≡CH); ^{13}C NMR (125 MHz, $CDCl_3$), δ 165.8, 164.4, 162.4, 162.2, 129.8, 129.5, 127.1, 118.5, 116.9, 78.9, 75.5, 64.5, 58.2, 43.0; HRMS (ESI) calculated for $C_{13}H_{11}FN_2O_4S$ $[M + H]^+$, m/z 311.0496; found, 311.0493.

2.4. General Synthetic Procedures for the Negative Probe (NP). Sodium hydroxide (120 mg, 3 mmol) dissolved in 5 mL of distilled water was added to a solution of probe **1** (465 mg, 1.5 mmol) in 5 mL of tetrahydrofuran (THF). The reaction was stirred at room temperature (RT) for 2 h. The mixture was acidified with dilute HCl to pH 4−5 and extracted with 20 mL of CH_2Cl_2 2 times. The organic layer was evaporated, and the crude product was purified by silica gel column chromatography with ethyl acetate/petroleum ether (1:6, v/v) to give the pure NP.

5-(4-Fluoro-3-((prop-2-yn-1-yloxy)methyl)phenyl)-1,3,4-oxadiazol-2-ol (NP): yield, 85%; white solid; ^{1}H NMR (500 MHz, DMSO-d_6), δ 12.60 (s, 1H, −OH), 7.84 (d, J = 6.8 Hz, 1H, Ph−6H), 7.79 (m, 1H, Ph−2H), 7.39 (t, J = 8.8 Hz, 1H, Ph−5H), 4.64 (s, 2H, Ph−CH_2O−), 4.26 (d, J = 2.4 Hz, 2H, −OCH_2−C≡CH), 3.51 (t, J = 2.4 Hz, 1H, −C≡CH); ^{13}C NMR (125 MHz, $CDCl_3$), δ 163.6, 161.5, 154.7, 154.6, 128.0, 127.5, 126.3, 120.2, 116.4, 79.0, 75.3, 64.6, 58.0; HRMS (ESI) calculated for $C_{12}H_9N_2O_3F$ $[M - H]^-$, m/z 247.0513; found, 247.0523.

2.5. *In Vitro* Antibacterial Bioassay. In this study, the antibacterial activities of target probes against *Xoo* and *Xac* were screened by a turbidimeter test. About 40 μL of liquid nutrient broth (NB) (1 g of yeast powder, 3 g of beef extract, 10 g of glucose, 5 g of peptone, and 1 L of distilled water at pH 7.0−7.2) containing *Xoo* or *Xac* was added to 5 mL of NB media containing the test compounds as experimental groups and dimethyl sulfoxide (DMSO) as a blank control. The inoculated test tubes were incubated at 28 ± 1 °C with a constant shake at 180 rpm until the bacteria reached the logarithmic growth phase. The growth of the culture was monitored on a microplate reader by measuring the optical density at 600 nm (OD_{600}). The *in vitro* inhibition rate, I (%), is calculated by the formula described below, where C represents the corrected absorbance value (OD_{600}) of the

DOI: 10.1021/acs.jafc.9b02059
J. Agric. Food Chem. 2019, 67, 6962−6969

DMSO NB media and T represents the corrected absorbance value (OD_{600}) of the compound-treated NB media.

$$\text{inhibition rate, } I\ (\%) = (C - T)/C \times 100$$

The half-maximal inhibitory concentration (IC_{50}) was determined from the equation via software SPSS 17.0. Each experiment was repeated 3 times.

2.6. Cell Culture. *Xoo* strain PXO99A and *Xac* strain *Xac* 29-1 cells were cultured in liquid NB medium (3.0 g of beef extract, 5.0 g of peptone, 1.0 g of yeast powder, and 10.0 g of glucose added to 1 L of distilled water at pH 7.0−7.2) at 28 °C for 12 h. Cells were cultivated in a constant temperature shaker with a speed of 180 rpm.

2.7. Preparation of Proteomes for *In Vitro* Experiments. *Xoo* or *Xac* cells were cultured in 1 L of liquid NB medium at 28 °C until OD_{600} reached 0.6 and then harvested by centrifugation at 6000 rpm. The bacterial cell pellet was washed with phosphate-buffered saline (PBS) 3 times, resuspended in 40 mL of PBS (pH 7.2) buffer, and lysed by sonication with a VCX150 (Sonics) instrument under ice cooling. The cell mixture was separated by centrifugation at 12 000 rpm for 45 min, and the protein concentration of the supernatant was determined by the Bradford assay, which was further adjusted to 1 mg/mL by dilution with PBS and stored at −80 °C until use.

2.8. *In Vitro* Labeling of Bacterial Proteomes. Proteome samples (44 μL of 1 mg/mL protein in PBS) were treated with 1 μL of desired concentrations of probe **1** or **2** for 2 h at 25 °C. For competition experiments with compound **0**, proteomes (43 μL) were first incubated with various concentrations of **0** (1 μL) for 2 h at 25 °C, followed by the addition of probe **1** (5 μM) or **2** (50 μM) for another 2 h. After incubation, 1 μL of biotin azide reagent (200 μM) was added, followed by 1 μL of freshly prepared sodium ascorbate solution (5 mM). Samples were gently vortexed, and the cycloaddition was initiated by the addition of 3 μL of a $CuSO_4$/2-(4-((bis((1-*tert*-butyl-1*H*-1,2,3-triazol-4-yl)methyl)amino)methyl)-1*H*-1,2,3-triazol-1-yl)acetic acid (BTTAA) mixture. A 50 mM BTTAA solution was preincubated with 50 mM $CuSO_4$ solution (2:1, v/v) before use. The reaction mixtures were then incubated at 37 °C for 2 h in the dark. After CC, 50 μL of 2× SDS loading buffer was added to the mixture to stop the reaction, which was further heated at 95 °C for 10 min. A total of 10 μg of protein per lane was loaded and separated by sodium dodecyl sulfate polyacrylamide gel electrophoresis (SDS−PAGE).

2.9. *In Situ* Labeling of Living Cells. *Xoo* or *Xac* cells were grown to OD_{600} = 0.6 in liquid NB medium at 28 °C. The growth media was removed by centrifugation at 6000 rpm, followed by washing with PBS 3 times. The cell pellet was resuspended in 990 μL of PBS and treated with various concentrations of probes (10 μL) or equal DMSO control at 25 °C for 2 h. In the case of competitive ABPP experiments, cells were resuspended in 980 μL of PBS, preincubated with various concentrations of **0** (10 μL) at 25 °C for 2 h, and then treated with probe **1** (5 μM) or **2** (50 μM) at 25 °C for another 2 h. After incubation with probes, the supernatant was separated by centrifugation and excessive probes were further removed by washing the cell pellet with PBS 3 times. The cell pellet was lysed by sonication on ice in 100 μL of PBS, followed by centrifugation at 12 000 rpm for 30 min. The protein concentration of the supernatant was determined by the Bradford assay and diluted to 1 mg/mL in PBS. The follow-up steps were performed as described above.

2.10. Streptavidin Blot. Proteins on the SDS gel were transferred to a polyvinylidene fluoride (PVDF) membrane at 4 °C for 60 min. The membrane was further blocked in 5% nonfat dried milk solution for 2 h at room temperature. After washing with PBS with 0.05% Tween 20 (PBST), the membrane was incubated with streptavidin−horseradish peroxidase (HRP, Sangon Biotech, with 1:1000 dilution in 5% nonfat dried milk PBST solution) for 2 h at 4 °C and detected by enhanced chemiluminescence (ECL) western blotting detection reagents (Bio-Rad). The PVDF membranes were scanned using the ChemiDoc XRS+ system (Bio-Rad).

2.11. Biotin−Streptavidin Enrichment Experiments. After the *in situ* labeling experiments as described above, the cell pellet was resuspended with PBS and lysed by sonication on ice. The supernatant was separated by centrifugation, and the protein concentration was measured by the Bradford assay, which was further adjusted to the same concentration. To 950 μL of supernatant, 10 μL of biotin azide (200 μM), 10 μL of sodium ascorbate solution (5 mM), and 30 μL of premixed $CuSO_4$/BTTAA solution were added, followed by incubation at 37 °C for 2 h. The reaction was then quenched by the addition of 4 mL of pre-chilled acetone. After incubation at −80 °C overnight, the mixture was subsequently centrifuged at 12 000 rpm for 15 min to obtain precipitated proteins. The supernatant was removed, and the precipitate was washed with pre-chilled MeOH thrice. The pellet was air-dried and resuspended in 1 mL of 0.2% SDS by sonication. Subsequently, the supernatant was incubated with 1 mL of prewashed streptavidin beads (Promega) for 2 h. After enrichment, beads were washed with 1% SDS/PBS, 6 M urea, and PBS. A total of 50 μL of 2× SDS loading buffer was added to the beads, which was further heated at 95 °C for 10 min to release the target proteins from the beads. The supernatant was collected by centrifugation and subjected to a preparative SDS gel. The enriched bands were visualized by Coomassie Blue staining.

2.12. In-Gel Digestion Analysis and Target Identification. The protein band on the SDS gel was excised and cut into 1 mm^2 pieces using a razor blade. The gel pieces were washed with double-distilled water (ddH_2O) and 100 mM ammonium bicarbonate and dehydrated with 100% CH_3CN, which were further reduced by 10 mM dithiothreitol (DTT) for 45 min at 37 °C with gentle shaking. Then, the gel pieces were alkylated by 55 mM iodoacetamide for 1 h at 37 °C in the dark. For trypsin digestion, 0.5 μg of trypsin (Promega) in 100 μL of 25 mM ammonium bicarbonate was added and the reaction was incubated at 37 °C overnight. The tryptic peptides were further separated by centrifugation and analyzed using a nano-liquid chromatogram coupled with TripleTOF 5600 MS (AB SCIEX). The mass spectrometry data were searched using the MaxQuant software (version 1.5.2.8) against the corresponding *Xanthomonas* proteome of the UniProt database. For protein modifications, N-terminal acetylation and oxidation on methionine were chosen as variable modification and carbamidomethylation on cysteine was chosen as fixed modification. Mass tolerances of the precursor and fragment ions were set to 6 and 20 ppm. The false discovery rates for peptide and protein identification were set to 1%.

2.13. Western Blot. After the enrichment experiment by streptavidin beads, proteins on the SDS gel were transferred on to a PVDF membrane, which was further blocked in 5% nonfat dried milk solution for 2 h. After washing with PBST, the membrane was incubated with primary rabbit polyclonal anti-dihydrolipoamide *S*-succinyltransferase (DLST) antibody (Wuhan GeneCreate Biological Engineering Co., Ltd., with 1:2000 dilution in 5% milk in PBST) for 2 h at 4 °C, followed by PBST washing. Subsequently, goat anti-rabbit immunoglobulin G (IgG) HRP-conjugated secondary antibody (Bio-Rad, with 1:2000 dilution in 5% nonfat dried milk PBST solution) was added, and the membrane was incubated at 4 °C for 2 h. Finally, the membrane was washed with PBST, and signals were detected by ECL western blotting detection reagents (Bio-Rad) using the ChemiDoc XRS+ system (Bio-Rad).

2.14. Cloning and Recombinant Expression of DLST (UniProt: A0A0K0GL90). The DLST gene (*sucB*) with *Nde*I/*Xho*I restriction enzyme sites was cloned into the pet-28a (+) plasmid vector by ligation independent cloning using the following primers: DLST-pET-28a (+) forward, CGCGGCAGCCATATGGCCACCGAAGTTAAAGTTCC; DLST-pET-28a (+) reverse, TGGTGGTGCTCGAGTTACAGACCAAACAGCATAC.

The DLST-pET-28a (+) construct was transformed into *Escherichia coli* BL21 cells for expression and selected on lysogeny broth (LB) agar plates with a 50 μg/mL concentration of kanamycin. Cells were incubated with kanamycin (50 μg/mL) at 37 °C until an OD_{600} of 0.6. Then, isopropyl β-D-thiogalactopyranoside (IPTG, 500 μM) was added to induce protein expression. Bacteria were harvested, and the cell pellet was then resuspended in lysis buffer, followed by sonication (30% power for 30 min) on ice. The mixture was separated by centrifugation, and the supernatant was loaded on a pre-equilibrated 5 mL HisTrap HP column (GE Healthcare). DLST was purified via a linear gradient elution with buffer A (50 mM Tris−HCl at pH 8.0, 100 mM NaCl, 50

DOI: 10.1021/acs.jafc.9b02059
J. Agric. Food Chem. 2019, 67, 6962−6969

Scheme 1. Synthetic Route of 0-Derived Probes

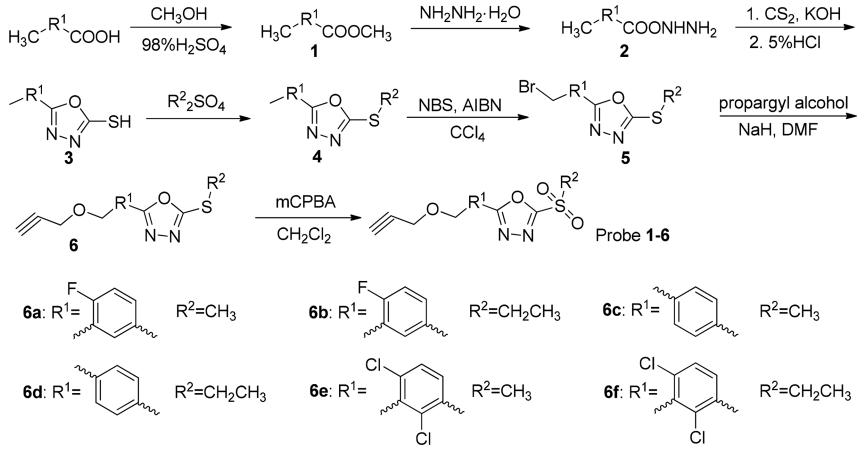

mM imidazole, 5% glycerol, and 1 mM DTT) and buffer B (50 mM Tris−HCl at pH 8.0, 100 mM NaCl, 400 mM imidazole, 5% glycerol, and 1 mM DTT) using an Äkta purifier system (GE Healthcare). Fractions containing DLST were pooled, concentrated, and digested by thrombin for 4 h, followed by further purification with a HisTrap column. Finally, fractions containing DLST were concentrated and adjusted to a concentration of 1 mg/mL for *in vitro* labeling experiments and then stored at −80 °C.

2.15. *In Vitro* Labeling of Recombinant DLST. A total of 50 ng of recombinant DLST (in 44 μL of PBS) was treated with the desired concentration of probe **1** (1 μL), and the reaction was incubated at 25 °C for 2 h. In the competition experiment, 50 ng of recombinant DLST was pretreated with different concentrations of **0** at 25 °C for 2 h, followed by the addition of 5 μM probe **1** for another 2 h. The followed steps were described as above.

2.16. Adenosine Triphosphate (ATP) Content Detection. Then, 5 mL of each cell culture (OD_{600} = 0.2) was incubated with the desired concentration of **0** at 28 °C for 2 h with the speed of 180 rpm. After incubation, the cells were harvested by centrifugation and washed with PBS. The pellet was resuspended with lysis buffer from the ATP detection kit and lysed by sonication (30% power) on ice. The supernatant was separated by centrifugation, and ATP content was determined by the luciferin−luciferase bioluminescence assay kit following the kit literature (Beyotime, China).

3. RESULTS AND DISCUSSION

3.1. Antibacterial Activity Test of Probes 1−6. To unravel the biological targets of **0**, we introduced a short alkyne tag to its benzene ring to synthesize a series of sulfone probes (Scheme 1). Also, we designed a NP for control experiments, which was synthesized by probe **1** under an intense base condition (Scheme 2). To test whether the structural

Scheme 2. Synthetic Route of NP

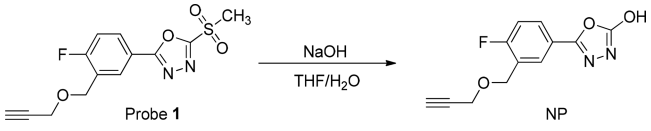

modifications influence the antibacterial activity of all probes, we determined their individual half-maximal inhibitory concentration (IC_{50}) against *Xoo* and *Xac* (Table 1) by a turbidimeter test, as described previously.[8] As expected, all probes showed good antibacterial activity against *Xoo* and *Xac*, suggesting that the addition of the clickable alkyne tag does not interfere with drug antibacterial activity. Notably, the antibacterial activity of probe **1** (IC_{50} = 3.58 μM) against *Xoo* was similar to **0** (IC_{50} = 3.51 μM), and the antibacterial activity of probe **2** (IC_{50} = 7.06 M) against *Xac* was slightly better than **0** (IC_{50} = 8.59 μM). Probes **1** and **2** perfectly keep the antibacterial activity of **0**, which is a prerequisite for ABPP target discovery. Meanwhile, the NP showed a dramatic drop in potency (IC_{50} > 500 μM) in both *Xoo* and *Xac* compared to **0**, thereby implying that the sulfonyl group may be critical for its antibacterial activity.

3.2. Target Analysis in *Xoo* and *Xac* by Probes 1 and 2. We next tested whether these probes are cell-permeable and can label enzymes in living pathogens. In this study, 5 μM probes **1**−**6** and 50 μM probes **1**−**4** were incubated with *Xoo* and *Xac* cells for 2 h, respectively. The subsequent cell lysis and CC with biotin azide were followed by SDS−PAGE analysis. Analysis of the labeled proteins by streptavidin blot detection showed a major band at ∼45 kDa (Figure S1 of the Supporting Information) in both *Xoo* and *Xac*, thereby indicating that these probes can enter the cells. All probes exhibited similar target preferences, thereby indicating that protein labeling is primarily driven by the scaffold rather than the attached modifications. In accordance with their activity, probe **1** showed a higher reactivity with p45 than probes **2**−**6** in *Xoo* cells and probe **2** outbalanced others in the *Xac* cells. Therefore, we used probes **1** and **2** to conduct all subsequent studies as a representative example.

To evaluate the reactivity of the probes, probe **1** was used to treat *Xoo* cellular lysates and living cells and probe **2** was used for *Xac* labeling experiments with different concentrations. Both *in vitro* and *in situ* studies of *Xoo* have shown that the labeling intensity of p45 increased over the concentration of probe **1**, which indicated a dose-dependent manner with p45 (Figure 2A). An intense labeling of this band could be observed as low as 2.5 μM, thereby indicating a high-affinity binding of p45 with probe **1**. Moreover, probe **1** demonstrated a distinct selectivity with p45 in *Xoo* cells. As shown in Figure 2A, labeling of *Xoo* lysates resulted in a much higher background and relative weaker labeling intensity compared to *Xoo* cells at the same concentration of probe **1**, thereby emphasizing the significance of *in situ* labeling as a precondition for specific target identification. Consistent with probe **1**, probe **2** also showed good target selectivity for p45 at a low concentration in *Xac* labeling experiments. Both *in vitro* and *in situ* studies of *Xac* have revealed a dose-dependent manner with p45, and even in a high concentration of 100 μM, p45 was identified as an undoubted major target (Figure 2B).

DOI: 10.1021/acs.jafc.9b02059
J. Agric. Food Chem. 2019, 67, 6962−6969

Table 1. Antibacterial Activities of 0 and 0-Derived Probes against *Xoo* and *Xac in Vitro*

	Xoo			*Xac*		
compound	regression equation	r	IC_{50} (μM)	regression equation	r	IC_{50} (μM)
0	$y = 7.64x + 5.53$	0.98	3.51 ± 0.04	$y = 4.39x + 3.61$	0.99	8.59 ± 0.16
probe **1**	$y = 10.40x + 4.51$	0.99	3.58 ± 0.03	$y = 3.75x + 2.24$	0.97	17.53 ± 0.10
probe **2**	$y = 7.53x + 1.90$	0.98	7.95 ± 0.09	$y = 2.55x + 4.08$	0.99	7.06 ± 0.25
probe **3**	$y = 28.44x - 0.92$	0.99	5.51 ± 0.03	$y = 1.93x + 3.73$	0.97	15.60 ± 0.14
probe **4**	$y = 27.40x - 12.27$	0.99	13.94 ± 0.03	$y = 2.34x + 3.62$	0.98	12.63 ± 0.33
probe **5**	$y = 4.19x + 4.33$	0.99	3.99 ± 0.08			
probe **6**	$y = 4.80x + 3.05$	0.98	6.80 ± 0.16			
NP			>500			>500

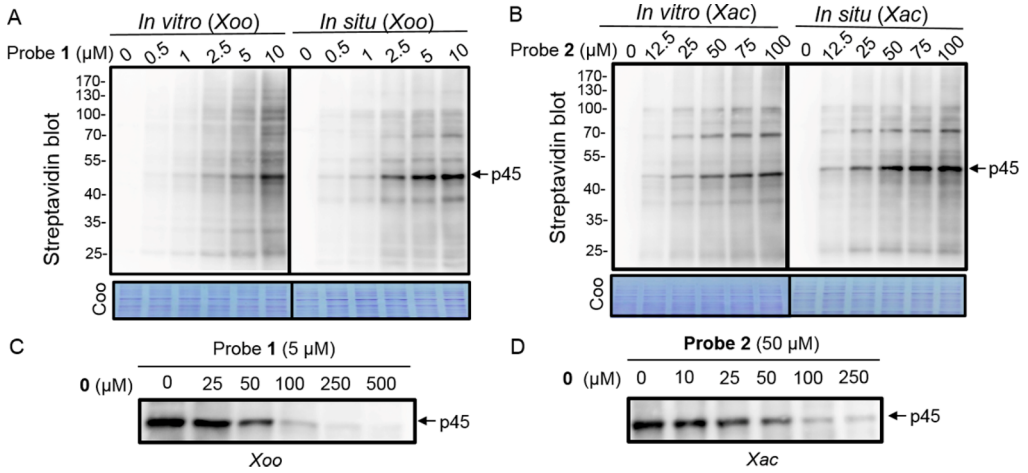

Figure 2. *In vitro* and *in situ* labeling of bacterial pathogens by the **0**-derived probes. Dose response of *in vitro* and *in situ* labeling revealed the potential engagement of probes (A) **1** and (B) **2** to an unknown target of ~45 kDa (p45) in both *Xoo* and *Xac*. Coo, Coomassie Blue staining shows protein loading. Dose-dependent blockade of labeling of p45 by pretreatment with **0** in (C) *Xoo* and (D) *Xac* cells. (A–D) Gel analysis by streptavidin blot.

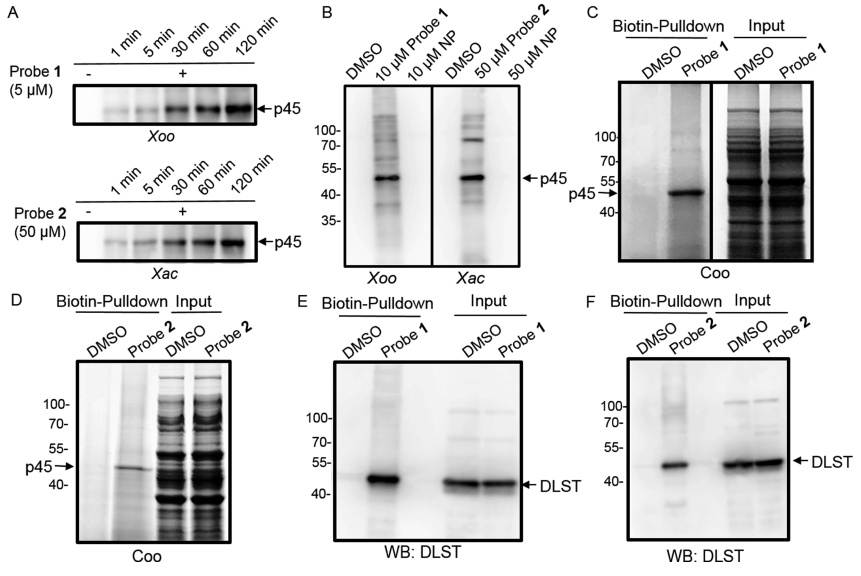

Figure 3. Kinetic analysis, covalent reaction, and target identification of DLST in *Xoo* and *Xac*. (A) Time-course experiments revealed a time-dependent manner with p45. (B) *In situ* labeling of *Xoo* and *Xac* by probes **1** and **2** and NP indicated a crucial role of the sulfonyl group for the labeling ability of the probes. (A and B) Gel analysis by streptavidin blot. (C) Streptavidin pull-down experiment by probe **1** enriched p45 in *Xoo* cells. (D) Streptavidin pull-down experiment by probe **2** enriched p45 in *Xac* cells. (C and D) Gel analysis by Coomassie Blue staining. Immunoblot analysis using an antibody confirmed that the protein pulled down by probes (E) **1** and (F) **2** was DLST. (E and F) Gel analysis by western blot.

To test whether the probes specifically interact with p45, we conducted *in vitro* and *in situ* competitive experiments with the pretreatment of **0**. By treating *Xoo* cells with **0** at the indicated concentrations for 2 h before the addition of 5 μM probe **1**, we measured an approximate IC_{50} value of 50 μM for **0** labeling of p45 (Figure 2C). Preincubation with 100 μM **0** resulted in a total loss of labeling signals, thereby indicating that **0** and the corresponding probe compete for the same binding sites.

DOI: 10.1021/acs.jafc.9b02059
J. Agric. Food Chem. 2019, 67, 6962–6969

Table 2. Results of Gel-Based Protein Identification of the p45 Band of *Xoo* Labeled with 100 μM Probe 1

			intensity			
Uniprot accession	protein name	MW (kDa)	DMSO (1)	DMSO (2)	probe **1** (1)	probe **1** (2)
A0A0K0GL90	dihydrolipoamide *S*-succinyltransferase	42.1	5.97×10^4	6.07×10^4	6.47×10^6	6.52×10^6

Consistent with the *in situ* labeling, we also found that pretreatment with **0** in *Xoo* cellular lysates abolished this labeling event with a similar potency to that detected in living cells (Figure S2A of the Supporting Information). In contrast, p45 again appeared to be a specific target in both *Xac* cells and lysates because its labeling signal was gradually reduced in the presence of an excess of **0** (Figure 2D and Figure S2B of the Supporting Information). Taken together, p45 is the specific and main target of **0** in both *Xoo* and *Xac*.

To visualize the rate of the labeling reaction, *Xoo* and *Xac* cells were incubated with sulfone probes for various incubation times. The cells were lysed by sonication and separated by centrifugation at 12 000 rpm, and the protein concentration was measured by the Bradford assay. After CC reaction with biotin azide and SDS−PAGE analysis, the labeled proteins were detected by streptavidin blot. As a result, we found that a detectable signal appeared within 5 min, indicating that the sulfone probes can be used for the rapid detection of p45 in living cells. In addition, the labeling intensity of p45 increased over time, which emphasizes that the probe binds to p45 in a time-dependent manner (Figure 3A).

3.3. Reactive Mode of Sulfone Probes with p45. As described above, the sulfone probes **1**−**6** showed good antibacterial activity against *Xoo* and *Xac*, while the NP probe almost showed no antibacterial activity. We speculated that the sulfonyl group is critical for the labeling ability of the probes. To test this hypothesis, 10 μM probe **1** and NP were used to treat *Xoo* cells. Furthermore, 50 μM probe **2** and NP were used for *Xac* cells, followed by CC reaction and streptavidin blot. Interestingly, probes **1** and **2** strongly labeled p45, and no labeling event was detected by NP, even at the concentration of 50 μM (Figure 3B), indicating that the oxadiazole ring was covalently attacked by the nucleophilic residues of protein targets and the sulfonyl group served as a leaving group. This result was in accordance with the reactivity of sulfone reagents as reported previously, thereby emphasizing the crucial role of the sulfonyl group for labeling protein targets.[5−7] When the sulfonyl group is substituted, the probe cannot react with the nucleophilic residue of target proteins and the corresponding antibacterial activity was significantly decreased.

3.4. Target Identification by MS Analysis and Validation by Western Blot. After these initial experiments, we next aimed to identify the p45 protein by a chemical proteomics approach. We treated *Xoo* and *Xac* cells with 100 μM probe **1** and 200 μM probe **2** for 2 h, separately, followed by lysis and CC reaction. The target proteins were affinity-purified by streptavidin beads, separated by SDS−PAGE, and stained by Coomassie Blue. As a result, probes **1** and **2** strongly purified p45 in both *Xoo* and *Xac* cells (panels C and D of Figure 3). The p45 band was then diced and subjected to in-gel trypsin digestion.[20,21] The resulting peptides were analyzed by liquid chromatography−tandem mass spectrometry (LC−MS/MS), and DLST was identified as the likely target of sulfone probes (Table 2 and Table S1 of the Supporting Information). As expected, the intensity of p45 in the probe **1** treated group is much higher than the DMSO control. The predicted molecular weight of DLST is 42.3 kDa, which is in accordance with the major labeling band detected in all labeling experiments.

To further validate the MS results, we implemented target enrichment by a pull-down experiment that was then applied to western blot analysis[22] using the DLST antibody. For anti-DLST western blot, the enriched target protein was prepared in the identical way as biotin−streptavidin enrichment experiments, as described above. After SDS−PAGE, proteins were transferred onto a PVDF membrane, blocked with 5% nonfat dried milk solution, and incubated with anti-DLST antibody, followed by the incubation with goat anti-rabbit IgG HRP-conjugated secondary antibody. The signals were detected by ECL western blotting detection reagents. As a result, an intense labeling band appeared in the probe-treated sample but not in the DMSO control, indicating that purified p45 by probes **1** and **2** was DLST (panels E and F of Figure 3). These results have confirmed DLST as the target of probe **1** in *Xoo* and probe **2** in *Xac*.

3.5. *In Vitro* Interaction of Probe 1 with Recombinant DLST. For additional validation experiments, recombinantly expressed DLST (from *Xoo*) was labeled by probe **1** in a dose-dependent manner, and no labeling event was detected by NP (Figure 4A). The labeling of DLST was markedly decreased with

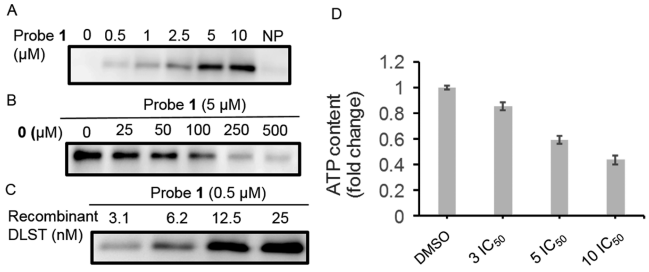

Figure 4. Labeling of recombinant DLST and its functional study by **0**. (A) Dose-dependent labeling of recombinant DLST with probe **1**. (B) Increasing concentrations of **0** prevented labeling of recombinant DLST with probe **1**. (C) Labeling of different concentrations of recombinant DLST indicated a high sensitivity with probe **1**. (A−C) Gel analysis by streptavidin blot. (D) Equant *Xoo* cells were treated with the concentrations of 0−10 IC_{50} of **0**, resulting in a dramatic decrease of the ATP content. Error bars represent standard deviation in three independent replicates.

a preincubation of excess **0**, thereby suggesting a specific interaction of DLST with probe **1** (Figure 4B). For the sensitivity detection experiment, a series of concentrations of recombinant DLST was incubated with probe **1** for 2 h. After CC reaction and streptavidin blot, we showed that probe **1** is highly sensitive for DLST, with a detection limit of 3.1 nM (Figure 4C). Furthermore, the labeling of DLST was completely blocked by preincubation with phenylmethylsulfonyl fluoride (PMSF) (Figure S3 of the Supporting Information), which is a known active-site inhibitor of serine proteases,[23] thereby indicating that probe **1** may covalently bind to the serine residues. Among these results, we have unambiguously confirmed that DLST is the target of probe **1** in cells.

DOI: 10.1021/acs.jafc.9b02059
J. Agric. Food Chem. 2019, 67, 6962−6969

3.6. Functional Study of DLST by 0. DLST is the structural and catalytic core of the 2-oxoglutarate dehydrogenase complex (KGDHC),[24] which catalyzes the oxidative decarboxylation of 2-oxoglutarate to succinyl-CoA and acts as a key regulatory enzyme of energy production in the tricarboxylic acid (TCA) cycle.[25] To date, efficacious and selective DLST inhibitors are unavailable and the functional studies of DLST were mostly conducted by genetic approaches.[26−28] To determine whether the inhibition of DLST will alter the energy production in cells, we treated *Xoo* cells with various concentrations of **0** and determined the ATP content by the luciferin−luciferase bioluminescence assay. As expected, the ATP content was decreased with the increase of **0** and resulted in more than a 40% decrease at the concentration of 10 IC_{50} compared to the DMSO control (Figure 4D). When DLST was inhibited, the energy production was interrupted, thereby indicating that compound **0** may serve as an effective tool for the functional study of DLST in bacteria.

In summary, we have developed a series of cell-permeable probes for target identification of bactericide **0** in living cells. Through chemical proteomic strategies, we validated DLST as an unprecedented target, which was also the first reported target of this novel structure. As a central enzyme in the TCA cycle, targeting this energy regulator may, therefore, represent an attractive strategy for antibacterial agent discovery. To date, the function of DLST remains largely unknown and was studied mostly by genetic approaches as a result of the lack of effective inhibitors. For the first time, we reported the covalent DLST inhibitor, the drug candidate **0**, which may serve as a useful tool for the functional study of DLST in cells. Taken together, we anticipate that target deconvolution of this sulfone-based antibacterial reagent may offer guidance for the discovery of novel agrochemicals.

■ ASSOCIATED CONTENT

Supporting Information

The Supporting Information is available free of charge on the ACS Publications website at DOI: 10.1021/acs.jafc.9b02059.

In situ labeling of *Xoo* and *Xac* cells with **0**-derived probes (Figure S1), competitive experiments with **0** preincubation of living cells and cell lysates (Figure S2), competition experiment with excess PMSF abolishing the labeling of recombinant DLST (Figure S3), results of gel-based protein identification of the p45 band of *Xac* labeled with 200 μM probe **2** (Table S1), synthesis and characterization data for other target compounds, and ^{1}H and ^{13}C NMR and HRMS spectra (PDF)

■ AUTHOR INFORMATION

Corresponding Authors

*E-mail: basong@gzu.edu.cn.
*E-mail: jhzx.msm@gmail.com.

ORCID

Cai-Guang Yang: 0000-0001-5778-4422
Yonggui Chi: 0000-0003-0573-257X
Baoan Song: 0000-0002-4237-6167
Song Yang: 0000-0003-1301-3030

Funding

The authors acknowledge financial support by the Key Technologies R&D Program (2014BAD23B01), the National Natural Science Foundation of China (21877021 and 21662009), and the Research Project of Chinese Ministry of Education (213033A and 20135201110005).

Notes

The authors declare no competing financial interest.

■ ABBREVIATIONS USED

ABPP, activity-based protein profiling; *Xoo*, *Xanthomonas oryzae* pv. *oryzae*; *Xac*, *Xanthomonas axonopodis* pv. *citri*; CC, click chemistry; AIBN, azobis(isobutyronitrile); m-CPBA, 3-chloroperbenzoic acid; DLST, dihydrolipoamide *S*-succinyltransferase; BTTAA, 2-(4-((bis((1-*tert*-butyl-1*H*-1,2,3-triazol-4-yl)methyl)amino)methyl)-1*H*-1,2,3-triazol-1-yl)acetic acid

■ REFERENCES

(1) Lamberth, C.; Jeanmart, S.; Luksch, T.; Plant, A. Current Challenges and Trends in the Discovery of Agrochemicals. *Science* **2013**, *341*, 742−746.

(2) Sparks, T. C.; Lorsbach, B. A. Perspectives on the agrochemical industry and agrochemical discovery. *Pest Manage. Sci.* **2017**, *73*, 672−677.

(3) Croston, G. E. The utility of target-based discovery. *Expert Opin. Drug Discovery* **2017**, *12*, 427−429.

(4) Mansfield, J.; Genin, S.; Magori, S.; Citovsky, V.; Sriariyanum, M.; Ronald, P.; Dow, M.; Verdier, V.; Beer, S. V.; Machado, M. A.; Toth, I.; Salmond, G.; Foster, G. D. Top 10 plant pathogenic bacteria in molecular plant pathology. *Mol. Plant Pathol.* **2012**, *13*, 614−629.

(5) Zhang, D.; Devarie-Baez, N. O.; Li, Q.; Lancaster, J. R.; Xian, M. Methylsulfonyl Benzothiazole (MSBT): A Selective Protein Thiol Blocking Reagent. *Org. Lett.* **2012**, *14*, 3396−3399.

(6) Chen, X.; Wu, H.; Park, C. M.; Poole, T. H.; Keceli, G.; Devarie-Baez, N. O.; Tsang, A. W.; Lowther, W. T.; Poole, L. B.; King, S. B.; Xian, M.; Furdui, C. M. Discovery of Heteroaromatic Sulfones As a New Class of Biologically Compatible Thiol-Selective Reagents. *ACS Chem. Biol.* **2017**, *12*, 2201−2208.

(7) Matos, M. J.; Oliveira, B. L.; Martínez-Sáez, N.; Guerreiro, A.; Cal, P. M. S. D.; Bertoldo, J.; Maneiro, M.; Perkins, E.; Howard, J.; Deery, M. J.; Chalker, J. M.; Corzana, F.; Jiménez-Osés, G.; Bernardes, G. J. L. Chemo- and Regioselective Lysine Modification on Native Proteins. *J. Am. Chem. Soc.* **2018**, *140*, 4004−4017.

(8) Xu, W. M.; Han, F. F.; He, M.; Hu, D. Y.; He, J.; Yang, S.; Song, B. A. Inhibition of Tobacco Bacterial Wilt with Sulfone Derivatives Containing an 1,3,4-Oxadiazole Moiety. *J. Agric. Food Chem.* **2012**, *60*, 1036−1041.

(9) Li, P.; Yin, J.; Xu, W. M.; Wu, J.; He, M.; Hu, D. Y.; Yang, S.; Song, B. A. Synthesis, Antibacterial Activities, and 3D-QSAR of Sulfone Derivatives Containing 1, 3, 4-Oxadiazole Moiety. *Chem. Biol. Drug Des.* **2013**, *82*, 546−556.

(10) Li, P.; Shi, L.; Yang, X.; Yang, L.; Chen, X. W.; Wu, F.; Shi, Q. C.; Xu, W. M.; He, M.; Hu, D. Y.; Song, B. A. Design, synthesis, and antibacterial activity against rice bacterial leaf blight and leaf streak of 2,5-substituted-1,3,4-oxadiazole/thiadiazole sulfone derivative. *Bioorg. Med. Chem. Lett.* **2014**, *24*, 1677−1680.

(11) Gao, M. N.; Yu, L.; Li, P.; Song, X. P.; Chen, Z.; He, M.; Song, B. A. Label-free quantitative proteomic analysis of inhibition of *Xanthomonas axonopodis* pv. *citri* by the novel bactericide Fubianezuofeng. *Pestic. Biochem. Physiol.* **2017**, *138*, 37−42.

(12) Li, P.; Hu, D. Y.; Xie, D. D.; Chen, J. X.; Jin, L. H.; Song, B. A. Design, Synthesis, and Evaluation of New Sulfone Derivatives Containing a 1,3,4-Oxadiazole Moiety as Active Antibacterial Agents. *J. Agric. Food Chem.* **2018**, *66*, 3093−3100.

(13) Evans, M. J.; Cravatt, B. F. Mechanism-Based Profiling of Enzyme Families. *Chem. Rev.* **2006**, *106*, 3279−3301.

(14) Barglow, K. T.; Cravatt, B. F. Activity-based protein profiling for the functional annotation of enzymes. *Nat. Methods* **2007**, *4*, 822−827.

(15) Cravatt, B. F.; Wright, A. T.; Kozarich, J. W. Activity-Based Protein Profiling: From Enzyme Chemistry to Proteomic Chemistry. *Annu. Rev. Biochem.* **2008**, *77*, 383−414.

DOI: 10.1021/acs.jafc.9b02059
J. Agric. Food Chem. 2019, 67, 6962−6969

(16) Sanman, L. E.; Bogyo, M. Activity-Based Profiling of Proteases. *Annu. Rev. Biochem.* **2014**, *83*, 249−273.
(17) Rostovtsev, V. V.; Green, L. G.; Fokin, V. V.; Sharpless, K. B. A Stepwise Huisgen Cycloaddition Process: Copper(I)-Catalyzed Regioselective "Ligation" of Azides and Terminal Alkynes. *Angew. Chem.* **2002**, *114*, 2708−2711.
(18) Speers, A. E.; Adam, G. C.; Cravatt, B. F. Activity-Based Protein Profiling in Vivo Using a Copper(I)-Catalyzed Azide-Alkyne [3 + 2] Cycloaddition. *J. Am. Chem. Soc.* **2003**, *125*, 4686−4687.
(19) Zheng, B.; DeRan, M.; Li, X.; Liao, X.; Fukata, M.; Wu, X. 2-Bromopalmitate Analogues as Activity-Based Probes To Explore Palmitoyl Acyltransferases. *J. Am. Chem. Soc.* **2013**, *135*, 7082−7085.
(20) Shevchenko, A.; Tomas, H.; Havli, J.; Olsen, J. V.; Mann, M. In-gel digestion for mass spectrometric characterization of proteins and proteomes. *Nat. Protoc.* **2006**, *1*, 2856−2860.
(21) Qian, Y.; Schürmann, M.; Janning, P.; Hedberg, C.; Waldmann, H. Activity-Based Proteome Profiling Probes Based on Woodward's Reagent K with Distinct Target Selectivity. *Angew. Chem., Int. Ed.* **2016**, *55*, 7766−7771.
(22) Chen, Y. C.; Backus, K. M.; Merkulova, M.; Yang, C.; Brown, D.; Cravatt, B. F.; Zhang, C. Covalent Modulators of the Vacuolar ATPase. *J. Am. Chem. Soc.* **2017**, *139*, 639−642.
(23) Böttcher, T.; Sieber, S. A. *β*-Lactones as Privileged Structures for the Active-Site Labeling of Versatile Bacterial Enzyme Classes. *Angew. Chem., Int. Ed.* **2008**, *47*, 4600−4603.
(24) Knapp, J. E.; Mitchell, D. T.; Yazdi, M. A.; Ernst, S. R.; Reed, L. J.; Hackert, M. L. Crystal structure of the truncated cubic core component of the Escherichia coli 2-oxoglutarate dehydrogenase multienzyme complex. *J. Mol. Biol.* **1998**, *280*, 655−668.
(25) Anderson, N. M.; Mucka, P.; Kern, J. G.; Feng, H. The emerging role and targetability of the TCA cycle in cancer metabolism. *Protein Cell* **2018**, *9*, 216−237.
(26) Yang, L.; Shi, Q.; Ho, D. J.; Starkov, A. A.; Wille, E. J.; Xu, H.; Chen, H. L.; Zhang, S.; Stack, C. M.; Calingasan, N. Y.; Gibson, G. E.; Beal, M. F. Mice deficient in dihydrolipoyl succinyl transferase show increased vulnerability to mitochondrial toxins. *Neurobiol. Dis.* **2009**, *36*, 320−330.
(27) Keßler, M.; Berger, I. M.; Just, S.; Rottbauer, W. Loss of dihydrolipoyl succinyltransferase (DLST) leads to reduced resting heart rate in the zebrafish. *Basic Res. Cardiol.* **2015**, *110*, 14.
(28) Anderson, N. M.; Li, D.; Peng, H. L.; Laroche, F. J. F.; Mansour, M. R.; Gjini, E.; Aioub, M.; Helman, D. J.; Roderick, J. E.; Cheng, T.; Harrold, I.; Samaha, Y.; Meng, L.; Amsterdam, A.; Neuberg, D. S.; Denton, T. T.; Sanda, T.; Kelliher, M. A.; Singh, A.; Look, A. T.; Feng, H. The TCA cycle transferase DLST is important for MYC-mediated leukemogenesis. *Leukemia* **2016**, *30*, 1365−1374.

DOI: 10.1021/acs.jafc.9b02059
J. Agric. Food Chem. 2019, 67, 6962−6969